

This is an author-created, un-copyedited version of an article accepted for publication in Nanotechnology. IOP Publishing Ltd is not responsible for any errors or omissions in this version of the manuscript or any version derived from it. The definitive publisher-authenticated version is available online at doi: [10.1088/0957-4484/21/44/445704](https://doi.org/10.1088/0957-4484/21/44/445704).

Finding a needle in a haystack: tip-enhanced Raman scattering for studying carbon nanotubes mixtures

K. L. Andrew Chan and Sergei G. Kazarian*

Department of Chemical Engineering, Imperial College London, SW7 2AZ, UK

Keywords: single wall carbon nanotubes; SWCNT; Confocal; Imaging; Contaminant; Detection

Abstract

Tip-enhanced Raman spectroscopy (TERS) has emerged as a powerful analytical tool for measuring chemical images with nanometer spatial resolution. In this paper, the application of TERS to study differentiation of SWCNT with 14 nm spatial resolution is demonstrated by the measurement of a mixture of two different types of SWCNT as the model sample. The results demonstrate that TERS is a viable tool for the detection and localisation of different SWCNT and amorphous carbon in mixed SWCNT based on the spectral differences in the radial breathing mode and the D bands.

1. Introduction

Raman microscopy is a powerful and valuable material characterisation method. Chemical images with Raman spectroscopy can be obtained by mapping point by point across a sample. The spatial resolution is limited by diffraction with a lateral resolution of $\sim 0.5 \mu\text{m}$ when measured in far-field confocal mode. To break the diffraction limit, a different approach has recently been developed by taking the advantage of surface enhanced Raman spectroscopy (SERS), which was discovered more than 30 years ago,[1] and atomic force microscopy (AFM). Tip-enhanced Raman scattering (TERS) has emerged as a promising technique that offers both rich chemical information and nanometer spatial resolution.[2-6] The idea of this approach is to probe samples using the surface enhanced Raman effects at the apex of a sharp AFM tip. Nanometer spatial resolution can be achieved by the extreme localised enhancement effect.[7, 8] Spatial resolution of $\sim 4 \text{ nm}$ has been reported based on

spectral shift of the G band of SWCNT when localised contact pressure was applied to the nanotube.[9] This opens up many opportunities in material analysis with vibrational spectroscopy for samples with nanoscale size domains. The synthesis of carbon nanotubes is a complicated process and impurities, such as other carbonaceous materials, are sometimes formed in the process.[10, 11] It has been shown that it is able to provide the complete atomic structural assignment of SWCNT based on the radial breathing mode (RBM) vibrational frequency.[12] Another work has demonstrated the chirality changes in SWCNT with 40 nm spatial resolution based on both the SWCNT G bands and RBM vibrations.[13] In this work, we demonstrate the possibility of detecting and locating different impurities in SWCNT bundles as well as differentiating a range of SWCNT using TERS. Because of the small distances between the SWCNT, their differentiation could not be performed using conventional Raman microscopy or imaging. Carbon nanotubes of different chiralities and diameters, d_t , have been deliberately mixed and used as model samples for this purpose. We also report on our approaches in TERS study using a commercial instrument[6] and the difference in performance on newly coated and recoated AFM tips.

2. Experimentals

TERS images were obtained with an inverted microscope with 100x oil immersion objective (NA of 1.3, Olympus), a Raman spectrometer (nVia Raman Microscope, Renishaw, UK) with 633 nm HeNe laser, a circular polariser (Renishaw, UK) and a 1024 x 400 pixels CCD (Andor detector) connected to an AFM system (NTEGRA Spectra, NTMDT). Contact mode Si AFM tips (CSG10, NTMDT) were sputtered with a thin layer of gold coating (K550X, Emitech, Quorum Technologies, UK) under the condition of 10^{-1} mbar of Argon, coating current of 35 mA, 45 mm distance from the sputtering source and 2 minutes of coating time. The soft piezo approach technique was adapted to avoid damage of the gold on the tip and the lowest contact pressure settings was used to minimise the impact between the tip and sample. The laser beam with a power of ~ 0.01 mW was focused on the sample and the apex of the gold coated AFM tip. A 0.3 s integration time was used to collect the Raman signal at each point of the map and data was collected at a rate of ~ 3 spectra per second. Data analysis was performed using the Nova software (NTMDT).

Two types of purified SWCNT were used in this study and were labelled as type A (HiPCo, Carbon Nanotechnology Inc.) and type B (P2-SWNT, Carbon Solutions). SWCNTs were sonicated in solvent (chloroform) for 10 minutes followed by spreading on a thin glass coverslip. The solvent was evaporated at room temperature. After all the solvent had evaporated, the coverslip with SWCNT was placed on the AFM stage which was integrated with the inverted microscope. An area with dispersed SWCNT was scanned using the

confocal Raman mode. The laser spot was positioned at the area that produced a strong SWCNT signal to ensure that some of the SWCNTs were illuminated within the laser spot. The illuminated area of the sample was then scanned by the gold coated AFM tip across the laser spot in contact mode. Whenever the tip entered the laser spot, an apparent increase in fluorescent background was noticed. In cases when the tip was TERS active, the area where SWCNT was present showed an enhanced Raman signal of the SWCNT. This is generally used as the “hot spot” for scanning. Figure 1 shows an example of a hot spot and the corresponding AFM image which were obtained simultaneously. The bright area in the Raman map coincides with the presence of SWCNT shown in the AFM image. The tip was fixed at the “hot spot” while TERS maps were obtained by moving the sample (maximum range is $\sim 100 \mu\text{m} \times 100 \mu\text{m}$).

3. Results and discussion

To demonstrate the TERS effect, an image of dispersed SWCNT (pure type A SWCNT) was first scanned with, then without tip. A chemical image of the SWCNT has been generated from the data by plotting the G-band intensity at 1596 cm^{-1} across the scanned area. The background is subtracted from the intensity image to remove the unwanted shift in baseline during measurements. The scan without the tip (tip retracted) shows a relatively broad feature with blurred edges (Figure 2B). The G band signal has ~ 40 counts under the defined measurement conditions. The image from the scan with tip in contact reveals sharper outlines of the SWCNT. An intensity profile across dispersed SWCNTs shows that the spatial resolution achieved was $\sim 14 \text{ nm}$. This was higher than previously reported[6] using a similar system apparently because of the smaller step size used in this experiment and was similar to the spatial resolution reported by others using different instruments.[14-16] The 4 nm spatial resolution reported by Yano et al[9] was achieved by measuring peak shift rather than Raman intensity and the high spatial resolution observed resulted from the mechanical effect on the sample under localised contact pressure. The enhanced spatial resolution compared to the far-field confocal measurement demonstrated in Figure 2 is the result of the localised enhancement of Raman intensity at the apex of the tip. Note that the G band intensity from the image with tip approached is ~ 120 counts which is $\sim 3\times$ the signal compared to the measurements without tip. On some occasions ($\sim 10\%$ of the tips), when a relatively high power laser was used ($\sim 1 \text{ mW}$) a very strong enhancement of Raman signal ($\sim 70\times$, comparing the G band intensity between tip being approached and retracted) from the tip can be observed. However, the signal decays rapidly when such strong enhancement occurs and eventually the entire enhancement is lost. The power of laser at the tip is important for experiments with longer acquisition time. The tip property was found to be changing continuously with higher laser intensities. The instability of the tip with high laser

power is thought to be caused by heating of the tip[17] which could induce physical instability of the gold coating. Under such condition, the gold coating may form shapes that can produce high TERS signal for a short period of time. When the gold coated tip is exposed in high laser intensity for a longer period of time (several minutes), the Si peak intensity from the AFM tip increases suggesting the gold is eventually evaporated resulting in a loss in TERS signal. Although the enhancement was very strong for those tips, it was not considered to be suitable for the scanning TERS experiment as a stable enhancement for a long exposure time under the laser light illumination is required. When weaker enhancement was observed, the enhanced signal was found to be more stable and the tip remained active for a few days as was the case with the results shown in Figure 2. When the enhancement is eventually lost due to wear or contamination of the tip (since the scan is operated in contact mode) the tip can be recoated by gold sputtering and the enhancement effect may be re-established. However, our experience has shown that the recoated tip often gives a lower enhancement level compared to newly coated tips, possibly due to the increased thickness of gold causing an increase in diameter of the recoated tip apex. Nevertheless, a strong enhancement is not a requirement for studying SWCNT. In our setup, the maximum laser power that can be used before the tip becoming unstable was ~ 0.05 mW. To prolong the life of an active tip, 0.01 mW laser power was used and the result obtained has shown that this level of laser power is sufficient for mapping SWCNT. In fact, the image shown in Figure 2A contains both far-field as well as TERS signals. Apparently, a clear TERS image of SWCNT can be produced with the current level of enhancement. From the Raman spectrum of the pure type A nanotube shown in Figure 3A, several bands in the RBM region can be noticed suggesting that this SWCNT type, despite being purified, contains nanotubes of different diameters. Another scanning TERS map (see Figure 3B-D) of the pure type A SWCNT on a glass cover slip with smaller step size has revealed a heterogeneous distribution of nanotubes of different diameters, which was generated using the bands at 287 cm^{-1} and 264 cm^{-1} . This demonstrates that scanning TERS is suitable to detect different SWCNT with various diameters within a bundle.

After establishing a TERS image with the set up described, scanning TERS was applied to analyse SWCNT that were intentionally contaminated with a different SWCNT (type B). The spectrum of type B SWCNT was overlapped with the spectrum of type A in Figure 3A. The shape of the G bands indicates that type A is semiconducting SWCNT, while type B is metallic SWCNT.[18] The other main spectral differences between the two SWCNTs are at the RBM in the lower wavenumber regions due to the large difference in diameters between the two SWCNT.[12, 19] The diameter distribution of the type B SWCNT appears to be less diverse and the RBM has a wavenumber significantly lower than type A. These differences

in spectral features allow images corresponding to the distribution of the contaminated SWCNT to be generated. Figure 4 shows the result of the measurement of the “contaminated” SWCNT bundles. The AFM topography image shows the outline of the SWCNT (Figure 4A). However, it contains no chemical information that may be used to distinguish the two different SWCNT. The TERS image based on the G band (1596 cm^{-1}) clearly outlines all the SWCNT as shown in Figure 4B. The presence of SWCNT was detected and the location coincided well with the topography image. The tip used to obtain these images was a recoated tip and the level of enhancement is smaller than with a newly coated tip, as demonstrated in Figure 2A. The TERS image generated by the Raman band due to the RBM vibration at $\sim 173\text{ cm}^{-1}$, which is specific to the contaminant SWCNT (type B), reveals the location of this type of SWCNT (Figure 4C). Note that despite type A containing SWCNT of several diameters, in all the TERS maps of pure type A sample no SWCNT was found with Raman spectral band at $\sim 173\text{ cm}^{-1}$. From these images, one can deduce that the type B SWCNT mostly appeared at the peripheral area around the main bundle. The result demonstrates that chemically specific Raman spectra can help to identify different SWCNT in the mixture with spatial resolution similar to an AFM measurement. Note that due to the weaker enhancement level compared to the measurement shown in Figure 2, the far-field Raman signal is relatively stronger, especially in the area where the SWCNT bundle is thickest. However, the more dispersed SWCNT at the peripheral area of the bundle seems to be less affected by the far-field signal. A high TERS signal can be produced from a small bundle while the far field signal from the same bundle is very small. On the other hand, a similar level of TERS signal would be expected from a much larger bundle due to the small enhancement zone for TERS while the far field signal is relatively stronger for the larger bundle.

It is interesting to note that a few of the “SWCNT” that were detected in the TERS images did not appear on the AFM topography image (indicated by the white arrows in Figures 4B and C). One of the possible reasons for this is the temporary sticking of small SWCNT on the hot spot. This is characterised by the appearance of the enhanced signal in a straight horizontal line. Another possible reason is that the feature was too thin to be detected with the slow AFM scan. Under normal operation, the AFM system can detect thin samples such as single layer graphene. However, when the topographic image was recorded during TERS measurement, the peak to peak noise level was increased due to the slow scanning speed. Raman spectra extracted from the region indicated by the arrow in Figure 4B show an enhanced signal with a strong D band. When the D band at 1320 cm^{-1} was used to generate the TERS image, the line indicated by the white arrow in Figure 4B is more clearly seen in the image in Figure 4D. The higher intensity of the D band can be an indication of the

presence of amorphous carbon.[18, 20] The result suggests that the imaged area was contaminated with amorphous carbon, which may also explain the lack of SWCNT like topographic features in that area.

4. Conclusions

In conclusion, it has been shown that TERS is a very useful tool for chemical analysis of nanometer scale materials with a demonstrated spatial resolution of 14 nm. Relatively small enhancement (~three times) is shown to be adequate, even beneficial, for the imaging of SWCNT. Tip stability was found to decrease dramatically when a higher power laser was used. We have demonstrated the application of scanning TERS to detect and locate SWCNT of the same type but different diameters (a single batch) and the contaminant SWCNT near a bundle of different types of SWCNT. Nanosize amorphous carbon contaminant can also be detected using this method. Differentiation of carbon nanotubes with different diameters in a mixture was possible for the first time due to the chemical specificity of Raman scattering and high spatial resolution using a gold-coated AFM tip.

Acknowledgements

SGK acknowledges the research funding from the European Research Council under the *European Community's Seventh Framework Programme (FP7/2007-2013) / ERC advanced grant agreement n° [227950]* and we thank NT-MDT.

References

- [1] Jeanmaire D L and Van Duyne R P 1977 Surface Raman spectroelectrochemistry.1. Heterocyclic, aromatic, and aliphatic-amines adsorbed on anodized silver electrode *J. Electroanal. Chem.* **84** 1-20
- [2] Stockle R M, Suh Y D, Deckert V and Zenobi R 2000 Nanoscale chemical analysis by tip-enhanced Raman spectroscopy *Chem. Phys. Lett.* **318** 131-6
- [3] Yeo B S, Schmid T, Zhang W H and Zenobi R 2007 Towards rapid nanoscale chemical analysis using tip-enhanced Raman spectroscopy with Ag-coated dielectric tips *Analytical and Bioanalytical Chemistry* **387** 2655-62
- [4] Hartschuh A, Qian H, Georgi C, Bohmler M and Novotny L 2009 Tip-enhanced near-field optical microscopy of carbon nanotubes *Analytical and Bioanalytical Chemistry* **394** 1787-95
- [5] Roy D, Wang J and Welland M E 2006 Nanoscale imaging of carbon nanotubes using tip enhanced Raman spectroscopy in reflection mode *Faraday Discuss.* **132** 215-25
- [6] Kharintsev S S, Hoffmann G G, Dorozhkin P S, de With G and Loos J 2007 Atomic force and shear force based tip-enhanced Raman spectroscopy and imaging *Nanotechnology* **18** 315502

- [7] Zhang W H, Cui X D, Yeo B S, Schmid T, Hafner C and Zenobi R 2007 Nanoscale roughness on metal surfaces can increase tip-enhanced Raman scattering by an order of magnitude *Nano Lett.* **7** 1401-5
- [8] Pettinger B, Domke K F, Zhang D, Picardi G and Schuster R 2009 Tip-enhanced Raman scattering: Influence of the tip-surface geometry on optical resonance and enhancement *Surf. Sci.* **603** 1335-41
- [9] Yano T, Verma P, Saito Y, Ichimura T and Kawata S 2009 Pressure-assisted tip-enhanced Raman imaging at a resolution of a few nanometres *Nat. Photonics* **3** 473-7
- [10] Shelimov K B, Esenaliev R O, Rinzler A G, Huffman C B and Smalley R E 1998 Purification of single-wall carbon nanotubes by ultrasonically assisted filtration *Chem. Phys. Lett.* **282** 429-34
- [11] Medjo R E, Sendja B T, Mane J M and Ateba P O 2009 A study of carbon nanotube contamination by XANES spectroscopy *Phys. Scr.* **80** 6
- [12] Jorio A, Saito R, Hafner J H, Lieber C M, Hunter M, McClure T, Dresselhaus G and Dresselhaus M S 2001 Structural (n, m) determination of isolated single-wall carbon nanotubes by resonant Raman scattering *Phys. Rev. Lett.* **86** 1118-21
- [13] Anderson N, Hartschuh A and Novotny L 2007 Chirality changes in carbon nanotubes studied with near-field Raman spectroscopy *Nano Lett.* **7** 577-82
- [14] Steidtner J and Pettinger B 2008 Tip-enhanced Raman spectroscopy and microscopy on single dye molecules with 15 nm resolution *Phys. Rev. Lett.* **100** 4
- [15] Cancado L G, Hartschuh A and Novotny L 2009 Tip-enhanced Raman spectroscopy of carbon nanotubes *J. Raman Spectrosc.* **40** 1420-6
- [16] Anderson N, Hartschuh A, Cronin S and Novotny L 2005 Nanoscale vibrational analysis of single-walled carbon nanotubes *J. Am. Chem. Soc.* **127** 2533-7
- [17] Zhang W H, Schmid T, Yeo B S and Zenobi R 2008 Near-field heating, annealing, and signal loss in tip-enhanced Raman spectroscopy *J. Phys. Chem. C* **112** 2104-8
- [18] Jorio A, Pimenta M A, Souza A G, Saito R, Dresselhaus G and Dresselhaus M S 2003 Characterizing carbon nanotube samples with resonance Raman scattering *New Journal of Physics* **5** 17
- [19] Dresselhaus M S, Dresselhaus G, Saito R and Jorio A 2005 Raman spectroscopy of carbon nanotubes *Phys. Rep.-Rev. Sec. Phys. Lett.* **409** 47-99
- [20] Hayazawa N, Yano T, Watanabe H, Inouye Y and Kawata S 2003 Detection of an individual single-wall carbon nanotube by tip-enhanced near-field Raman spectroscopy *Chem. Phys. Lett.* **376** 174-80

500 nm

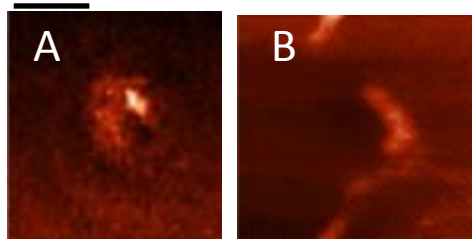


Figure 1: (A) Image of a hot spot based on the G band of SWCNT. (B) AFM topography measured simultaneously during scanning for the hot spot.

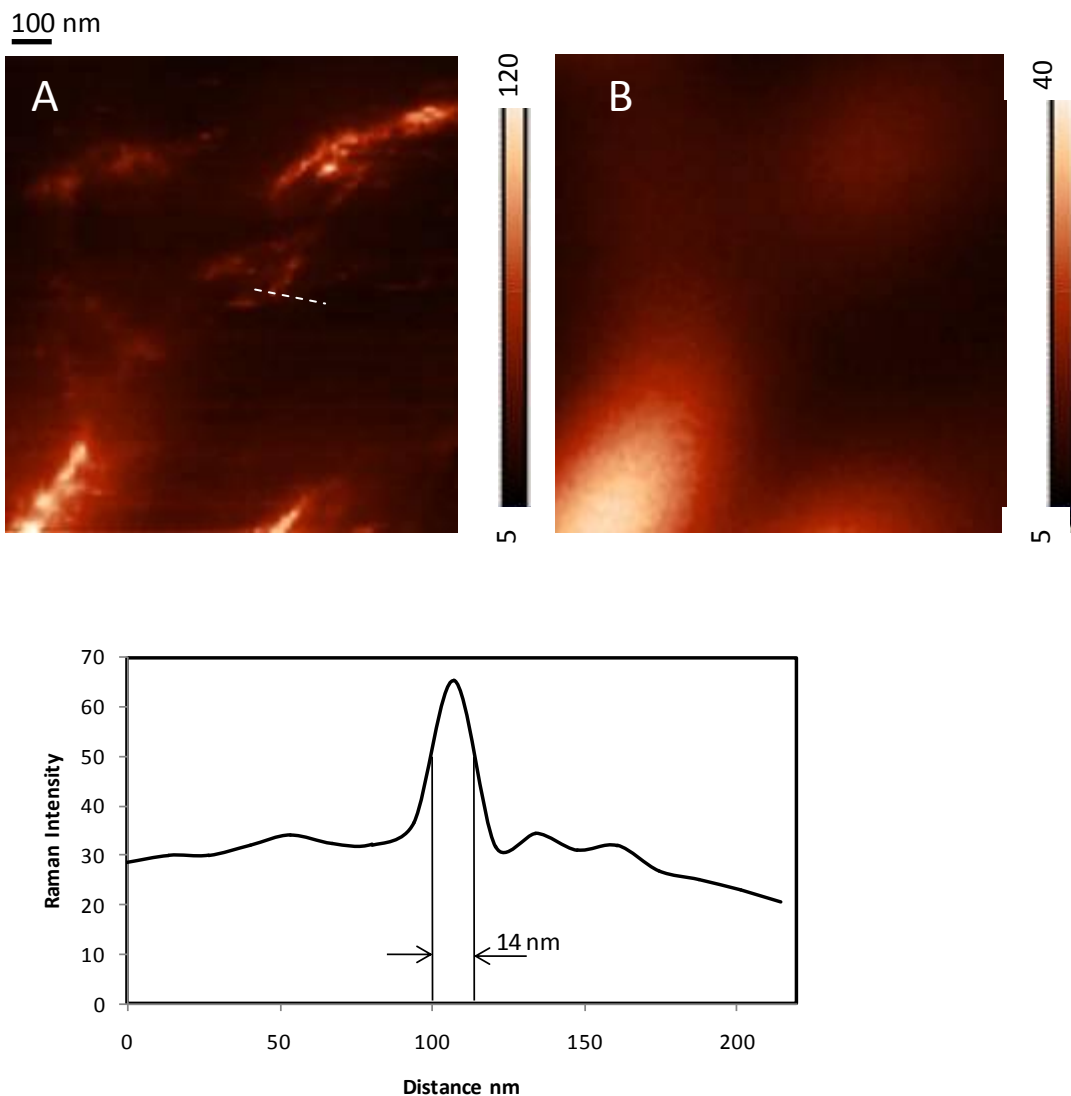
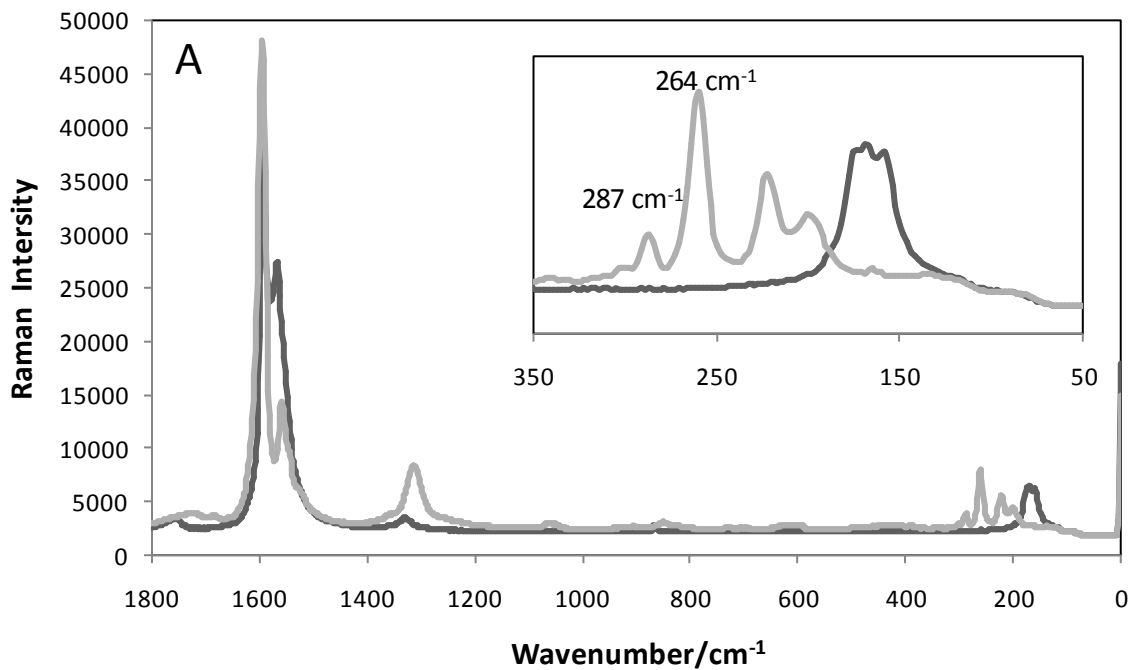


Figure 2: TERS image of dispersed SWCNT, type A. The images are generated based on the intensity of the SWCNT G band at 1596 cm^{-1} . Image A shows the result when tip is approached. Image B shows the result when tip is retracted. The plot has shown the Raman intensity profile along the dotted line marked on Figure 2A.



50 nm

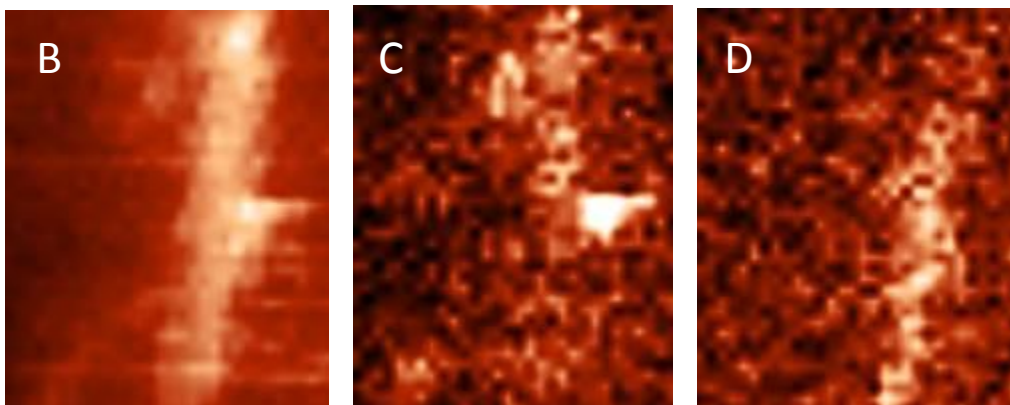


Figure 3: A) Raman spectra of type A (grey line) and type B (dark grey line) SWCNT measured using a confocal Raman microscope. The insert has shown the expanded spectral region for the RBM vibrations of the two SWCNT. B, C and D are the scanning TERS images of the dispersed pure type A SWCNT generated by plotting the intensity of the G-band (1595 cm^{-1}), the band from RBM at 287 cm^{-1} and 264 cm^{-1} across the measured area, respectively.

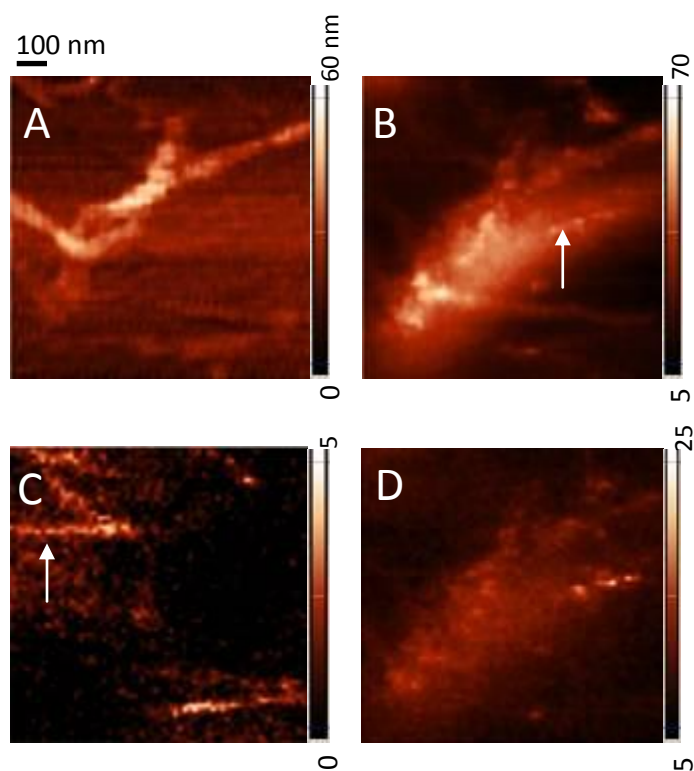


Figure 4: Images measured simultaneously with gold coated tip approached sample. (A) An AFM topographic image of the measured area of the dispersed SWCNT mixture. (B) TERS image of the SWCNT based on the G band at 1596 cm^{-1} . (C) TERS image of the SWCNT based on the radial breathing mode specific to the contaminant SWCNT at $\sim 173\text{ cm}^{-1}$ (Type B). (D) TERS image of the SWCNT based on the D band at $\sim 1320\text{ cm}^{-1}$ highlighting an area of amorphous carbon.